

# Development of data acquisition and over-current protection systems for a suppressor-grid current with a neutral-beam ion source

Wei LIU (刘伟)<sup>1,2</sup>, Chundong HU (胡纯栋)<sup>1</sup>, Sheng LIU (刘胜)<sup>1</sup>,  
Shihua SONG (宋士花)<sup>1</sup>, Jinxin WANG (汪金新)<sup>1</sup>, Yan WANG (王艳)<sup>1,2</sup>,  
Yuanzhe ZHAO (赵远哲)<sup>1</sup> and Lizhen LIANG (梁立振)<sup>1</sup>

<sup>1</sup>Institute of Plasma Physics Chinese Academy of Sciences, Hefei 230031, People's Republic of China

<sup>2</sup>University of Science and Technology of China, Hefei 230026, People's Republic of China

E-mail: [zyz@ipp.ac.cn](mailto:zyz@ipp.ac.cn)

Received 2 June 2017, revised 11 September 2017

Accepted for publication 12 September 2017

Published 25 October 2017



CrossMark

## Abstract

Neutral beam injection is one of the effective auxiliary heating methods in magnetic-confinement-fusion experiments. In order to acquire the suppressor-grid current signal and avoid the grid being damaged by overheating, a data acquisition and over-current protection system based on the PXI (PCI eXtensions for Instrumentation) platform has been developed. The system consists of a current sensor, data acquisition module and over-current protection module. In the data acquisition module, the acquired data of one shot will be transferred in isolation and saved in a data-storage server in a txt file. It can also be recalled using NBWave for future analysis. The over-current protection module contains two modes: remote and local. This gives it the function of setting a threshold voltage remotely and locally, and the forbidden time of over-current protection also can be set by a host PC in remote mode. Experimental results demonstrate that the data acquisition and over-current protection system has the advantages of setting forbidden time and isolation transmission.

Keywords: neutral beam injection, high-current ion source, suppression grid current, data acquisition and protection system

(Some figures may appear in colour only in the online journal)

## 1. Introduction

In order to support the physical research of the Experimental Advanced Superconducting Tokamak (EAST), two beamlines of neutral beam injection (NBI) have been developed [1–3]. The ion sources are the important part of the beamlines. Accelerator grids containing ion sources consist of a plasma grid (PG), gradient grid, suppressor grid (SG) and an exit grid.

There are two main functions of the SG with an ion source. The first is for the SG to prevent backstream electrons from getting into the ion source. The second is that the SG is helpful in establishing a stable optical system.

During the beam extraction, the abnormal beam optic will lead to an anabatic increase of SG current. The heat overload caused by backstream electrons will damage the accelerator grids. At the same time, the phenomenon of

overshoot of the SG current exists at the start of beam extraction, which will cause error protection. In order to obtain the SG current signal, protect the accelerator grids and avoid error protection, data acquisition and over-current. a protection system for an SG current has been developed.

The details of the data acquisition and over-current protection system are discussed as follows. The system structure design is shown in part 2, the experiential result is described in part 3 and the conclusion is given in part 4.

## 2. System structure design

The layout of the data acquisition and over-current protection system is shown in figure 1. The primary units of the data acquisition and over-current protection system are a current

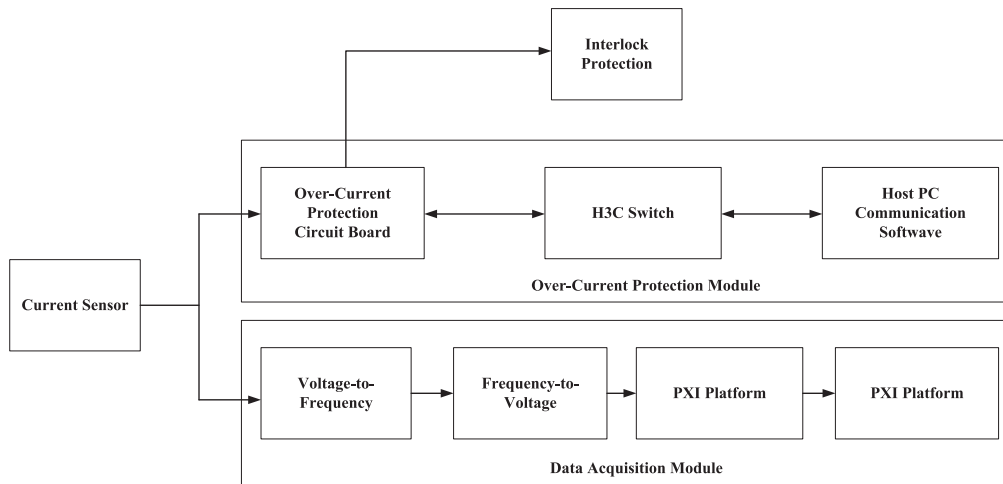


**Figure 1.** The block diagram of the data acquisition and over-current protection system.

sensor, data acquisition module and over-current protection module.

Pulse Step Modulator technology is used for the PG power supply, which consists of one hundred and forty-four modulators, and the voltage of one modulator is 780 V. The number of modulators added to the PG power supply, controlled by proportion integration differentiation, is determined by a setpoint [4]. The rising edge time of the SG power supply is faster than that of modulators, which causes unmatched electric-field intensity. As the unmatched electric-field intensity causes the phenomenon of overshoot of the suppression current at the start of beam extraction, the data acquisition and over-current protection system should contain the function of setting forbidden time.

Because of the complicated electric- and magnetic-field environment of the experimental lab, the SG current signal is not suitable for long-distance transmission directly. In order to achieve long-distance transmission, optic isolation transmission is adopted in the system. In the data acquisition module, voltage-to-frequency (VF) and frequency-to-voltage (FV) technology are used for isolation transmission with an optic fiber, which gives immunity to electromagnetic interference (EMI) and enhances the precision of the data acquisition.

### 2.1. Data acquisition hardware

The data acquisition module based on the PCI eXtensions for Instrumentation (PXI) platform contains VF and FV circuit boards that provide galvanic isolation and immunity to EMI and National Instruments (NI) PXI with the following parts [5]:

- PXIe-6535 (simultaneous sampling card) has advanced features to allow sample 32-CH differential analog inputs and 32-bit resolution at the maximum sampling rate of  $1 \text{ MS s}^{-1}$ ;
- PXI-1031(chassis);
- PXIe-8840(system controller) delivers ultimate performance for a wide variety of measurement applications

with a 2.6 GHz processor, and 4 G 1600 MHz DDR3 memory.

The voltage generated by the current sensor is obtained and converted to an optic frequency signal by the VF circuit board. The input range of the VF circuit is 0–10 V, which corresponds to a 0–1 MHz frequency signal. The optic frequency signal is transmitted to the FV circuit board by fiber. In the control room, the FV circuit board converts the optic frequency signal to a voltage signal with 0–10 V. The PXI platform acquires the voltage signal via the PXIe-6535 sampling card, and the signal is saved in the hard disc in a txt file. Operators can recall the data using NBWave, which is the graphical display software for the EAST NBI.

### 2.2. Over-current protection hardware

The over-current protection module consists of an over-current protection circuit board, H3C switch, and host PC. As shown in figure 2, the over-current protection circuit board consists of a microcontroller unit (MCU), Schmitt trigger, alarm circuit, LED segment displays, following circuit, watchdog timer, Ethernet circuit, trigger circuit and RS-232 interface used for the system debug.

In the process of the experiment, the over-current protection circuit board is the core of the system. Figure 3 gives the operations performed by the MCU and the logic used for the performance of its firmware. C is used as the programming language.

In remote mode, the 12-bit analog-to-digital converter (ADC) of the MCU converts the voltage signal generated by the current sensor into a digital code after forbidden time when the over-current protection circuit board receives the trigger signal. In order to ensure impedance matching between the current sensor and AD sampling circuit, the following circuit is adopted in the circuit board. If the voltage signal exceeds the threshold voltage, the MCU will send an alarm signal to the interlock protection via optic fiber. In order to reduce the influence of the EMI, the MCU averages the sample data after multiple samplings. The circuit board communicates with the host PC via the User Datagram

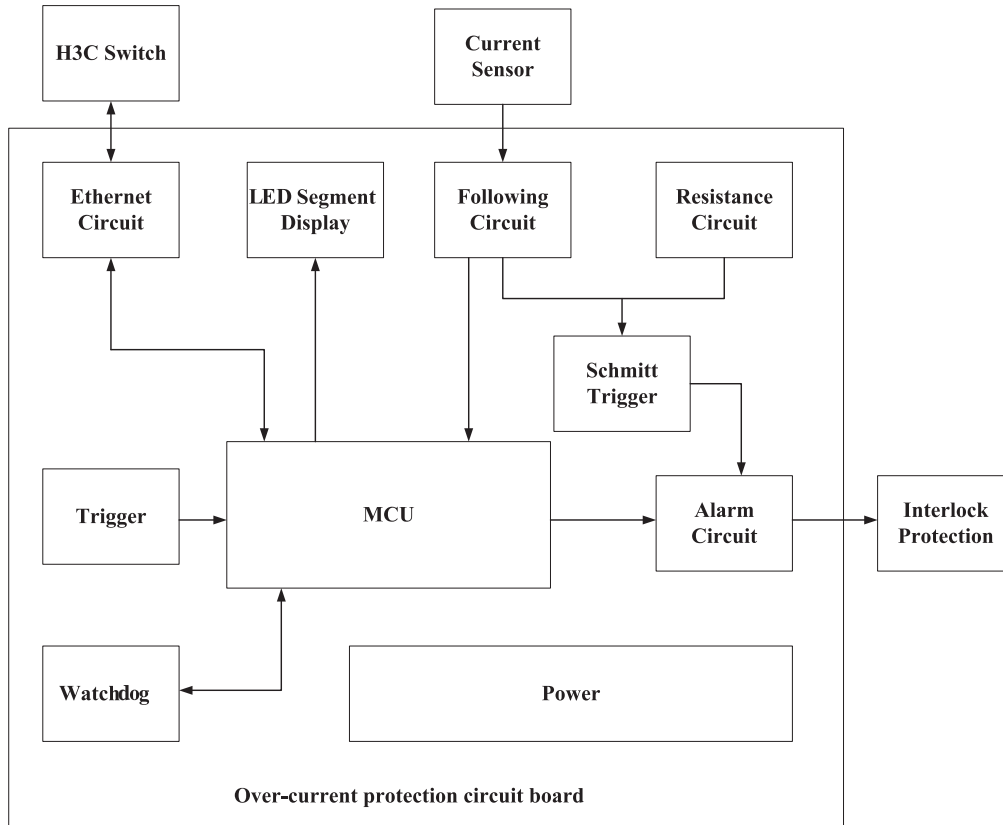


Figure 2. Block diagram of over-current protection circuit board.

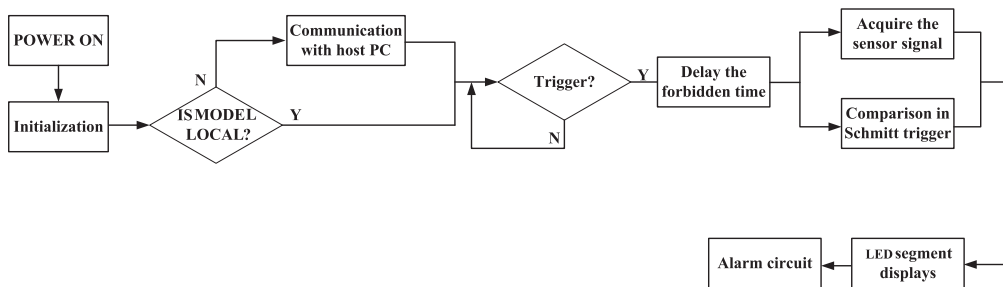


Figure 3. Logic operation of the over-current protection circuit board.

Protocol communication protocol. The threshold voltage number can be sent by the host PC in the control room. Meanwhile, the value of the SG current calculated by the MCU is shown in LED segment displays dynamically.

The W5500 chip adopted in the over-current protection circuit board is a hardwired TCP/IP (transmission control protocol/ internet protocol), and it is used as the primary chip in Ethernet communication [6]. The W5500 enables operators to have internet connectivity in their applications by using only a single chip in which the TCP/IP stack, 10/100 Ethernet MAC (media access control) and PHY (physical layer transceiver) are embedded. The Ethernet application can be put into use simply by loading the simple socket program. A Serial Peripheral Interface (SPI) is provided for easy connection with the MCU. The W5500's SPI supports 80 MHz speed and new efficient SPI protocol for high-speed network communication. In order to protect the Ethernet

communication circuit from electric surge, it should be connected to Ethernet by network transforms [7, 8].

In the local model, the threshold voltage is set by a resistance circuit and displayed in LED segment displays. As the complex electromagnetic environment causes the possibility of error trigger; in order to increase the reliability of over-current protection, a Schmitt trigger circuit has been chosen for the system [9]. The voltage generated by the current sensor is compared with the threshold voltage of the Schmitt trigger circuit. The Schmitt trigger circuit is shown in figure 4.

$V_{ref}$  stands for threshold voltage.  $R_1, R_2$  are the feedback resistances that are calculated by equations (1)–(3).  $V_{OH}$  and  $V_{OL}$  are the transistor–transistor logic (TTL) output levels (high or low).  $V_i$  is the input of the Schmitt trigger circuit.

$$V_{Thigh} = \frac{R_1}{R_2} \cdot V_{OL} + \frac{R_1 + R_2}{R_2} \cdot V_{ref} \quad (1)$$

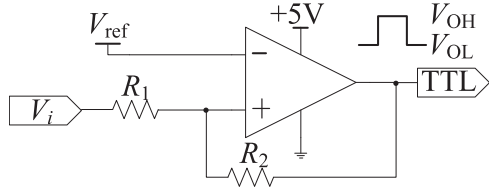


Figure 4. Circuit connection of Schmitt trigger.

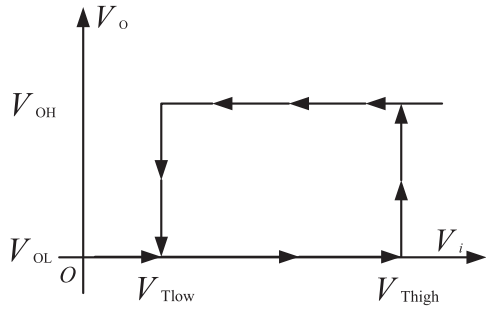


Figure 5. Transfer-characteristic curve of Schmitt trigger.

$$V_{Tlow} = \frac{R_1}{R_2} \cdot V_{OH} + \frac{R_1 + R_2}{R_2} \cdot V_{ref} \quad (2)$$

$$\Delta V = V_{Tlow} - V_{Thigh} = \frac{R_1}{R_2} (V_{OH} - V_{OL}). \quad (3)$$

In equations (1)–(3), the hysteresis interval is represented by  $\Delta V$ .  $V_{Thigh}$  and  $V_{Tlow}$  are the maximum and minimum input voltage that can trigger the alarm signal. The transfer-characteristic curve of the Schmitt trigger is shown in figure 5. The output level will change to become higher, when  $V_i > V_{Thigh}$ , when the alarm circuit is triggered and the alarm signal sent to the interlock protection module [10]. Conversely, the output level will become lower, when  $V_i < V_{Tlow}$ , when the Schmitt trigger will maintain stabilization during the hysteresis interval ( $\Delta V$ ) [11]. Hence, output level is kept steady during the  $\Delta V$ . The Schmitt trigger can reduce the proportion of error protection caused by electromagnetic noise effectively.

### 3. Experimental result

According to the experimental measurement, the forbidden time of over-current protection is 5 ms, which is the best choice. As shown in figure 6, CH1–CH4 represent the alarm signal, protection value, suppressor-current signal, and trigger signal, respectively. In the test diagram, the SG current signal (CH3) exceeds the protection value (CH2). The system receives the trigger signal (CH4) first, and then the alarm signal (CH1) will be sent after 5 ms.

Experimental results show that the system can work steadily in a practical environment. The acquired data of the SG current signal are further analyzed in MATLAB and shown in figure 7. The output voltage of the current sensor per ampere is  $1/3 \text{ V A}^{-1}$ . The SG current is converted into voltage by the current sensor and loaded into the Schmitt trigger circuit or the ADC of the MCU. If the voltage signal

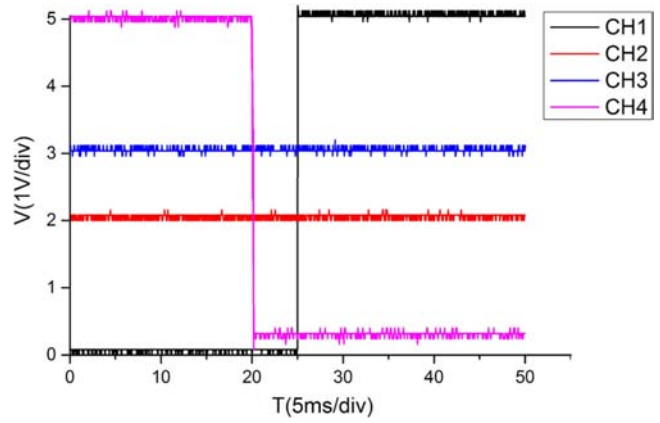


Figure 6. Test diagram of forbidden time.

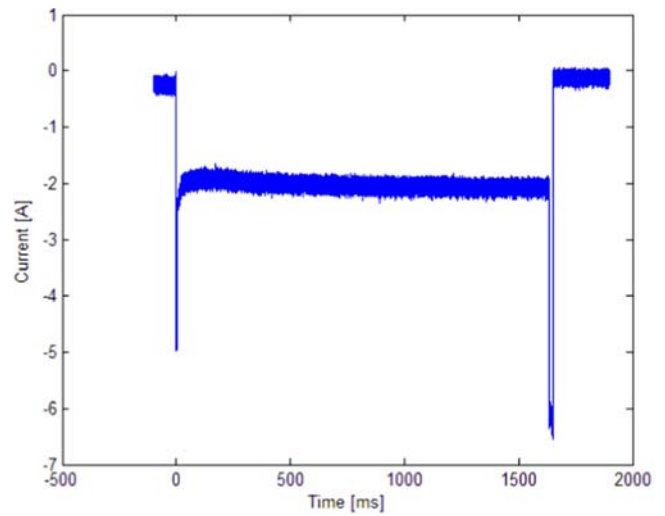
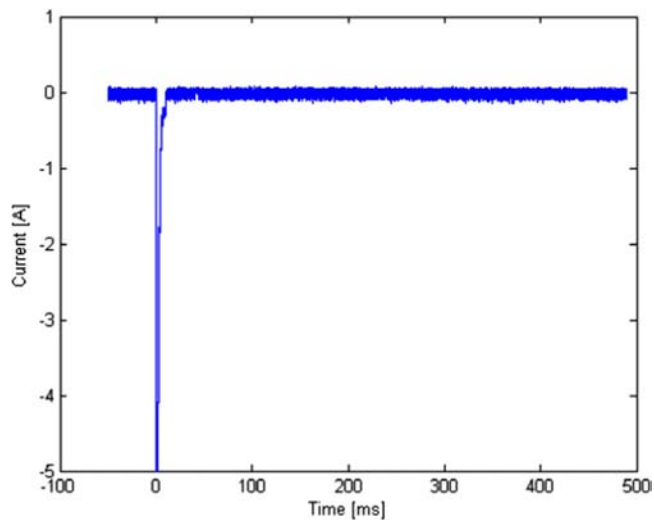


Figure 7. The protection system avoids the overshoot at the start of beam extraction, and the process is cut off when SG current exceeds the threshold voltage.

exceeds threshold voltage, the over-current protection module will send the alarm signal to the interlock protection system and cut off beam extraction [12]. In the process of the experiment, the threshold voltage is 1 V, which corresponds to 3 A of SG current. As shown in figure 7, the SG current is 5 A at the start of beam extraction. The over-current protection avoids error protection effectively. The system shuts down the beam extraction when the SG current is above 3 A. Because the system uses the method of multiple samplings, the protection time will delay by 17 ms, which is determined by the sampling number and sampling rate of the ADC of the MCU.

As shown in figure 8, the error protection is caused by overshoot at the start of beam extraction in the previous over-current protection, and the beam extraction is shut down by the error protection. If the over-current protection does not contain the function of forbidden time, the beam extraction will not work normally.



**Figure 8.** In the previous over-current protection, the overshoot exceeds the threshold voltage and causes error protection at the start of beam extraction.

#### 4. Conclusion

Experimental results show that the data acquisition and over-current protection system works well in terms of accuracy, stability, and also intelligence, which was used in experience

in BL-1. Owing to the number of advantages the system has, it will be put into operation in NBI BL-2 [13, 14].

#### Acknowledgments

This work is supported by National Natural Science Foundation of China (No.11575240), Key Program of Research and Development of Hefei Science Center, CAS (grant 2016HSC-KPRD002).

#### References

- [1] Chang D H et al 2011 *Fusion Eng. Des.* **86** 244
- [2] Hu C D et al 2015 *Plasma Sci. Technol.* **17** 817
- [3] Yahong X et al 2014 *Plasma Sci. Technol.* **16** 429
- [4] Kraus W et al 2015 *Fusion Eng. Des.* **91** 16
- [5] Kumar A et al 2016 *Fusion Eng. Des.* **112** 865
- [6] Mehta S et al 2017 *Opt. Switch. Netw.* **23** 52
- [7] Sardar B et al 2014 *J. Netw. Comput. Appl.* **41** 89
- [8] Lar S-U and Liao X 2013 *J. Netw. Comput. Appl.* **36** 126
- [9] Milecki A and Regulski R 2016 *Mech. Syst. Signal Process.* **78** 43
- [10] Khorami A and Sharifkhani M 2016 *AEÜ Int. J. Electron. C.* **70** 886
- [11] Azeemuddin S and Sayehb M R 2011 *Optik* **122** 1935
- [12] Hugues J A et al 2011 *Microelectron. J.* **42** 785
- [13] Hu C and NBI Team 2012 *Plasma Sci. Technol.* **14** 567
- [14] Hu C 2015 *Plasma Sci. Technol.* **17** 1